

## 論文の内容の要旨

### 光誘起相転移材料 $\lambda$ - $\text{Ti}_3\text{O}_5$ の光学特性 (Optical properties of a photo-induced phase transition material $\lambda$ - $\text{Ti}_3\text{O}_5$ )

氏名 箱江 史吉

#### Introduction

Our group recently reported a unique phase of titanium oxide  $\lambda$ - $\text{Ti}_3\text{O}_5$ .  $\lambda$ - $\text{Ti}_3\text{O}_5$  exhibits a photo-induced phase transition to  $\beta$ - $\text{Ti}_3\text{O}_5$  at room temperature (Figure 1). The phase transition was also observed by not only light irradiation but also applying pressure and heating.  $\lambda$ - $\text{Ti}_3\text{O}_5$  is dark blue and paramagnetic metallic conductor, while  $\beta$ - $\text{Ti}_3\text{O}_5$  is nonmagnetic semiconductor. Electric properties (electrical conductivity), optical properties (reflectance and transmittance) and magnetic properties (magnetic susceptibility) change during the phase transition. So,  $\lambda$ - $\text{Ti}_3\text{O}_5$  is an attractive material for such as switching devices, sensors and memory devices.

In this research, to demonstrate the reversible phase transition on  $\lambda$ - $\text{Ti}_3\text{O}_5$  by applying pressure and irradiating light, photo-irradiation effect on  $\beta$ - $\text{Ti}_3\text{O}_5$  which was produced by applying pressure on  $\lambda$ - $\text{Ti}_3\text{O}_5$  was investigated. Successively, it is necessary to synthesize a film of  $\lambda$ - $\text{Ti}_3\text{O}_5$  for the application to these devices, so the synthetic method of a  $\lambda$ - $\text{Ti}_3\text{O}_5$  film was studied. And then, the optical constants of  $\lambda$ - $\text{Ti}_3\text{O}_5$  were determined by spectroscopic ellipsometry.

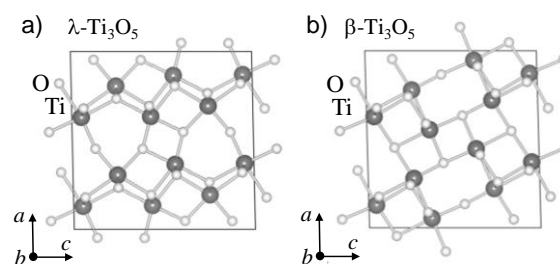


**Figure 1.** The crystal structure of a)  $\lambda$ - $\text{Ti}_3\text{O}_5$  and b)  $\beta$ - $\text{Ti}_3\text{O}_5$ . View of the unit cell in the  $ac$  plane. Black and white ball represent Ti and O atoms, respectively.

### Pressure and photo irradiation effect on $\lambda$ -Ti<sub>3</sub>O<sub>5</sub>

Pressure of 2.5 GPa was applied to flake form  $\lambda$ -Ti<sub>3</sub>O<sub>5</sub> for 10 minutes by a pellet-forming machine. Then, light irradiation was conducted by 532 nm nanosecond-pulsed laser light (6 ns,  $2.4 \times 10^{-6}$  mJ  $\mu\text{m}^{-2}$  pulse<sup>-1</sup>) to the sample. The changes of XRD pattern were measured during applying pressure and light irradiation repeatedly.

Applying pressure of 2.5 GPa, the XRD pattern of the sample showed pressure-induced phase transition from  $\lambda$ -Ti<sub>3</sub>O<sub>5</sub> to  $\beta$ -Ti<sub>3</sub>O<sub>5</sub> (Figure 2a). Then, irradiation with 532 nm nanosecond-pulsed laser caused an increase of  $\lambda$ -Ti<sub>3</sub>O<sub>5</sub> and a decrease of  $\beta$ -Ti<sub>3</sub>O<sub>5</sub> (Figure 2b). This result indicated that the  $\beta$ -Ti<sub>3</sub>O<sub>5</sub> which was produced by applying pressure on  $\lambda$ -Ti<sub>3</sub>O<sub>5</sub> returned to  $\lambda$ -Ti<sub>3</sub>O<sub>5</sub> by light irradiation. Furthermore, additional applying pressure of 2.5 GPa caused pressure-induced phase transition from  $\lambda$ -Ti<sub>3</sub>O<sub>5</sub> to  $\beta$ -Ti<sub>3</sub>O<sub>5</sub> again (Figure 2c). These phase transitions occurred repeatedly. This is the demonstration of the reversible phase transition between  $\lambda$ -Ti<sub>3</sub>O<sub>5</sub> and  $\beta$ -Ti<sub>3</sub>O<sub>5</sub> by pressure and light.

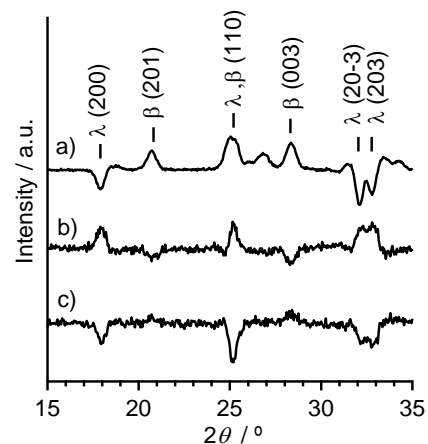


**Figure 2.** Difference XRD patterns of a) applying pressure of 2.5 GPa, b) 532 nm photo irradiation and c) applying pressure of 2.5 GPa again on the flake form  $\lambda$ -Ti<sub>3</sub>O<sub>5</sub>.

### Synthesis and optical properties of the $\lambda$ -Ti<sub>3</sub>O<sub>5</sub> film

A  $\lambda$ -Ti<sub>3</sub>O<sub>5</sub> film was prepared by the following procedure. Quartz substrate was treated with saturated potassium hydroxide water-ethanol solution beforehand. TiO<sub>2</sub> sol was coated on the quartz substrates by spin-coating method (1000 rpm, 10 second). The TiO<sub>2</sub> sol was 15 wt% anatase TiO<sub>2</sub> (particle size :  $3.3 \pm 0.9$  nm) dispersed in water. The obtained TiO<sub>2</sub> film was sintered at 1175 °C for five hours under H<sub>2</sub> flow (0.085 L/min). Then the sintered blue films was obtained. The thickness of the film was measured by a scanning electron microscope (SEM). The crystal structure was determined by X-ray diffraction (XRD) measurement. The optical properties of the sintered film were investigated by UV-vis transmission spectra and ellipsometric measurements. The ellipsometric measurements were conducted around the pseudo-Brewster's angle at the four angles of incidence (55 °, 60 °, 65 ° and 70 °).

According to cross sectional SEM image of the sintered film, the film thickness was  $100 \pm 20$  nm (Figure 3a). XRD pattern and Rietveld analysis of the sintered film indicated a monoclinic crystal structure (space group:  $C2/m$ ) with  $a = 9.848$  Å,  $b = 3.7836$  Å,  $c = 9.970$  Å and  $\beta = 91.08$  °, which were consistent with that of  $\lambda$ -Ti<sub>3</sub>O<sub>5</sub> reported previously (Figure 3b). Preferred orientation was observed with the (110) plane lying parallel to the plane of the substrate. The transmission spectrum of the sintered film showed a broad absorption around 900 nm (Figure 3c).

The ellipsometric data and the transmission spectrum of sintered film were analyzed by the three layers model of surface-roughness / film / substrate, whose dielectric constants were modeled by Gaussian model for electric transitions and Drude model for free carriers (Figure 4a, b). Then, the optical constants (the refractive index  $n$  and the extinction coefficient  $k$ ) of the  $\lambda$ -Ti<sub>3</sub>O<sub>5</sub> were estimated (Figure 4c). In the range of 350 -1700 nm, the values of

$n$  are 2.0 – 2.6, and the values of  $k$  are 0.1 – 0.8.

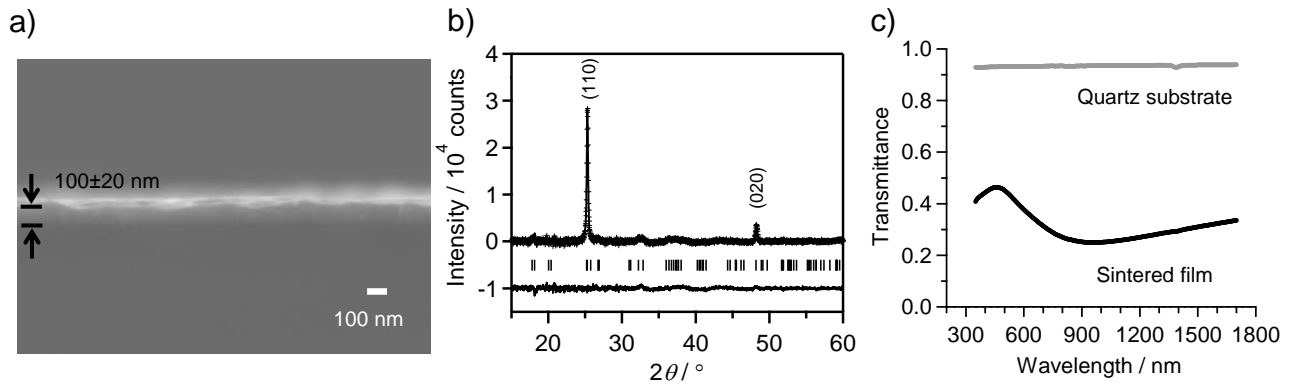


**Figure 3.** a) Cross sectional SEM image of the sintered film. b) XRD patterns and Rietveld analysis of the sintered film. Broad baseline caused by the quartz substrate was eliminated. Dots, line, lower line and bars represent the observed pattern, the calculated pattern, their difference and the Bragg reflections of  $\lambda$ -Ti<sub>3</sub>O<sub>5</sub>, respectively. c) Transmission spectra of quartz substrate (gray line) and the sintered film (Black line).

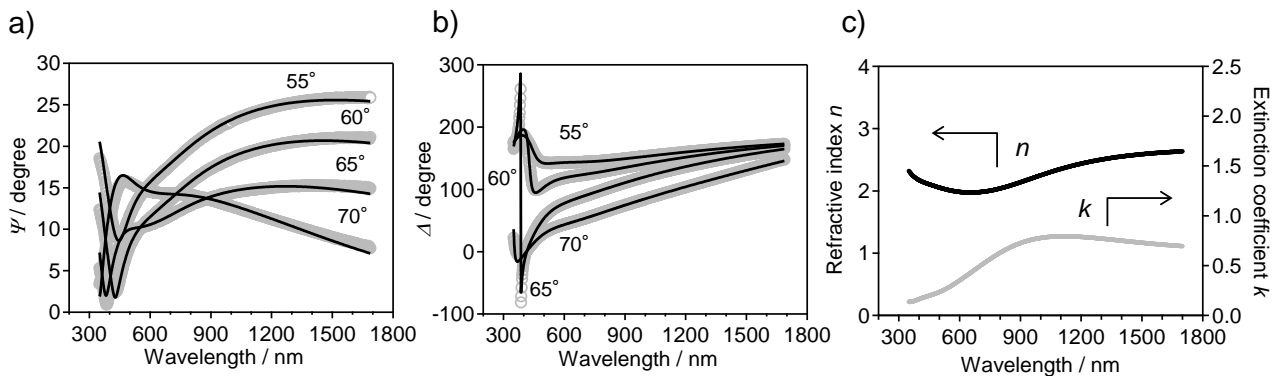


**Figure 4.** Ellipsometric analysis of the sintered film. a) The amplitude ratio  $\Psi$  and b) the phase difference  $\Delta$ . Gray dots and black line represent the observed ellipsometric data and the simulation, respectively. The angles of incidence are 55°, 60°, 65° and 70°. c) The optical constants of  $\lambda$ -Ti<sub>3</sub>O<sub>5</sub>. Black dots and gray dots indicate the refractive index  $n$  and the extinction coefficient  $k$ , respectively.

## Conclusion

In this research, photo-irradiation effect on  $\beta$ -Ti<sub>3</sub>O<sub>5</sub> which was produced by applying pressure on  $\lambda$ -Ti<sub>3</sub>O<sub>5</sub> was investigated, and the phase transitions between  $\lambda$ -Ti<sub>3</sub>O<sub>5</sub> and  $\beta$ -Ti<sub>3</sub>O<sub>5</sub> by pressure and light were demonstrated. In addition, the preparation method of a  $\lambda$ -Ti<sub>3</sub>O<sub>5</sub> film which is necessary for applying this material to the devices was studied. A film form of  $\lambda$ -Ti<sub>3</sub>O<sub>5</sub> was synthesized by sintering TiO<sub>2</sub> nanoparticles on quartz substrate under H<sub>2</sub> flow. And then, the optical constants,  $n$ ,  $k$ , of  $\lambda$ -Ti<sub>3</sub>O<sub>5</sub> which is useful to apply this material for optical devices were obtained by ellipsometric analysis of synthesized  $\lambda$ -Ti<sub>3</sub>O<sub>5</sub> film. These results contribute to revealing the physical properties of  $\lambda$ -Ti<sub>3</sub>O<sub>5</sub> as a functional material.